Supplementary Information (SI) for Journal of Materials Chemistry A.

Supporting Information

Radiation-cooled aramid composite films featuring tunable TiO_2 nanorod arrays anchored on the surface of 2D Mica nanosheet for passive daytime radiative cooling application

Bo Ma,[abc]† Wei Guo,[bc]† Jixiang Zhang,*[abc] Cui Liu,[bc] Nian Li,[bc] Shudong Zhang,*[bc] and Zhenyang Wang*[bc]

[a] School of Mechatronics and Vehicle Engineering, Chongqing Jiaotong University, Chongqing 400074, China.

[b] Institute of Solid State Physics, Hefei Institutes of Physical Science, Chinese Academy of Sciences, Hefei, 230031, China.

[c] Key Laboratory of Photovoltaic and Energy Conservation Materials, Hefei Institutes of Physical Science, Chinese Academy of Sciences, Hefei, 230031, China.

*Corresponding Authors

Email:zhangjixiang@163.com, sdzhang@iim.ac.cn, zywang@iim.ac.cn

Note S1: Experimental principles section

Step 1: Growth of TiO_2 seeds by hydrothermal method. $Ti(O\text{-}Bu)_4$ was hydrolysed to produce $Ti(OH)_4$, $Ti(OH)_4$ was deposited on Mica to form TiO_2 seeds. After the preparation of TiO_2-seeds, Mica still maintains its original two-dimensional structure with a large number of disordered and tightly arranged TiO_2 nanoparticles uniformly encapsulated on its surface, and its synthetic equation[1-2] is as follows:

$$Ti(O\text{-}Bu)_4 + 4H_2O \rightarrow Ti(OH)_4 \rightarrow TiO_2 \bullet nH_2O$$

Step 2: Growth of TiO_2 nanorods by Ti-H_2O_2 method,[3-5] the synthesis equation can be expressed as:

$$Ti + H_2O_2 \xrightarrow{HNO_3} [TiO(H_2O_2)]^{2+} \rightarrow Ti^{4+}(OH)_X \rightarrow H_2Ti_5O_{11} \bullet 3H_2O \rightarrow TiO_2$$

Metal Ti is eroded by H_2O_2 in acidic solution to form $Ti(OH)_4$, which is unstable at high temperatures and decomposes to form titanium dioxide sol. Dissolution of the formed titanium dioxide sol releases hydrated Ti(IV) ions into solution and once a critical concentration is reached, the hydrated Ti(IV) ions precipitate back into the Ti substrate to form titanium dioxide films. The additive HNO_3 affects the ‘directional attachment’ process of titanium dioxide, which in turn affects the resulting nanofeatures. The hydrolysis of melamine with the addition of HNO_3 generates NH^{4+}, the selective absorption of NH^{4+} on certain crystal surfaces of TiO_2, which contributes to the ‘directional attachment’ growth of $H_2Ti_5O_{11}$-$3H_2O$. [3, 5-6] The monoclinic crystal type $H_2Ti_5O_{11}$-$3H_2O$ was converted to rutile TiO_2 nanorods at 550 °C.

Step 3: ASCFs were produced by solvent exchange and deprotonation. Firstly, TiO_2 NAs-Mica was modified by APTES in order to make it have positive charge, and ANFs were deprotonated by DMSO and KOH in a mixture of solvents in order to make them have negative charge. Then, the APTES-modified TiO_2 NAs-Mica and ANFs were mixed and stirred for 2 h. IPA was slowly dripped in, and TiO_2 NAs-Mica was stacked into a layered structure by solvent exchange and turbulent shear,[7] finally ASCFs were prepared by vacuum filtration.

Note S2: Theoretically Calculated Radiative Cooling Power.

When the radiative cooler is placed horizontally on the ground and exposed to a cloudless sky, it's effected by the solar radiation and downward radiation from the atmosphere. The net cooling power P_{cool} can be calculated through the following equations:

$$P_{cool}(T) = P_{\gamma}(T) - P_a(T_a) - P_s(T) - P_c$$

$$P_{\gamma}(T) = A\int d\Omega \cos\theta \int_0^{\infty} d\lambda I_{BB}(T,\lambda)\varepsilon(\lambda,\theta)$$

$$P_a(T_a) = A\int d\Omega \cos\theta \int_0^{\infty} d\lambda I_{BB}(Ta,\lambda)\varepsilon(\lambda,\theta)\varepsilon_a(\lambda,\theta)$$

$$P_s = A\cos\theta_s \int_0^{\infty} d\lambda \varepsilon(\lambda,\theta_s) I_{AM1.5}(\lambda)$$

$$P_c(T,T_a) = Ah_c(T_a - T)$$

where T is the temperature of the radiative cooler, T_a is the temperature of the surrounding environment, P_{γ} is the power radiated by the cooler, P_a is the absorption of downward atmospheric thermal radiation, P_s is the absorbed solar power and P_c is the power lost due to the conductive and convective heat change with the surroundings, A, Ω and θ are surface area of the sample, a solid angle and angle between the solid angle and the normal direction of the sample's surface, respectively, ε(λ, θ) is emissivity of the object at a particular wavelength λ and angle θ ,$\varepsilon_{\alpha}(\lambda, \theta)$ is emissivity of the atmosphere, θ_s is the direction of the sunlight, h_c is nonradiative heat coefficient that is comprised of heat convection and heat conduction and its value ranges from 0 to 9 $W \cdot m^{-2} \cdot K^{-1}$.

Table S1 Compared the solar reflectance, IR emissivity, anti-UV and flexible of ASCFs with other reported cooling materials

Sample	Solar reflectance (%)	IR emissivity (%)	Anti-UV	Flexible
Siloxane coating[51]	92	93	Unknown	No
Polymethyl Methacrylate Film[52]	85	98	Unknown	Yes
Cooling wood[47]	96	90	No	No
Cellulose fabric[49]	91.7	90	No	Yes
PVA fabric[12]	94	94	Unknown	Yes
PEO fabric[54]	96	78	Unknown	Yes
MMA film[20]	95	98	Unknown	Yes
PU aerogel[55]	97	88	No	No
Cellulose paper[56]	95	93	No	Yes
Ceramic aerogel[57]	94	95	Unknown	No
PDMS coating[58]	90	92	Unknown	No
PDMS coating[48]	96	94	Unknown	No
Cellulose foam[13]	97	94.8	No	No
PEO/PT fabric[50]	94	91	Yes	Yes
PE fabric[53]	93	96	Yes	Yes
This work	97.5	96.3	96h UV	Yes

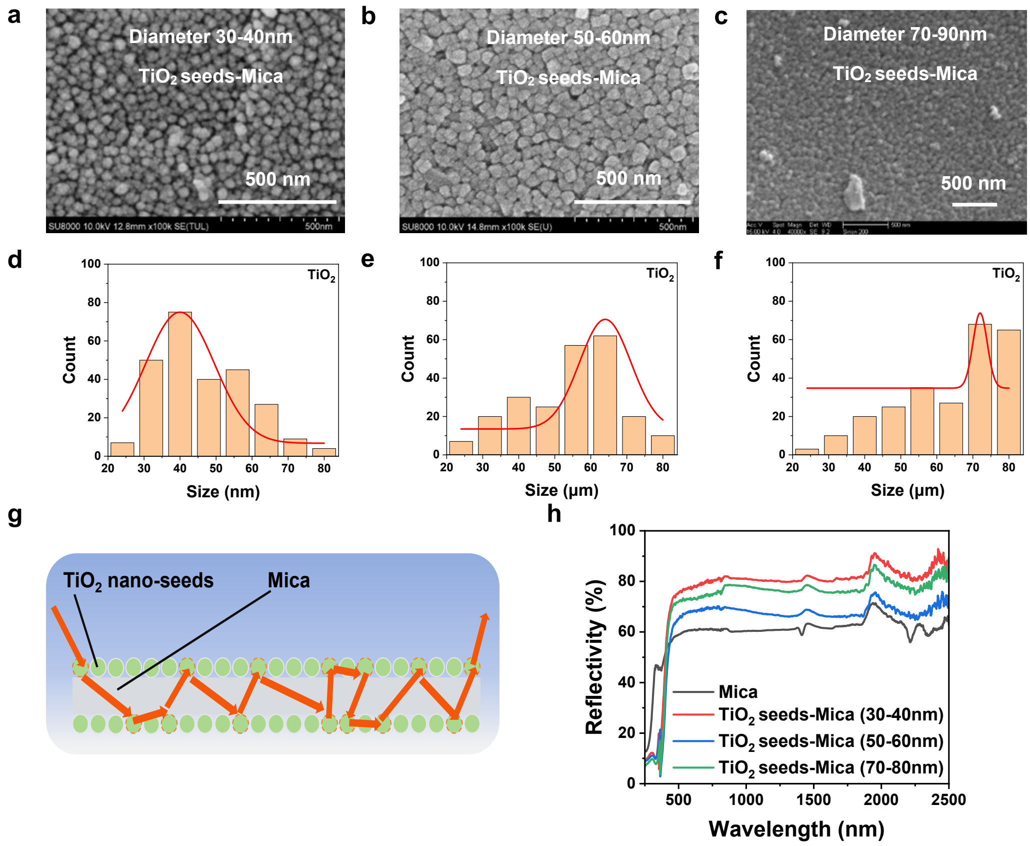

Fig. S1 Statistics of different TiO_2 seeds diameters and solar reflectance (TiO_2 seeds-Mica). (a-c) SEM images of TiO_2 seeds-Mica with different particle sizes. (d-f) Statistical plot of particle size of TiO_2 seeds-Mica. (g) Schematic Scattering of TiO_2 seeds-Mica. (h) Solar reflectance of different TiO_2 seeds-Mica.

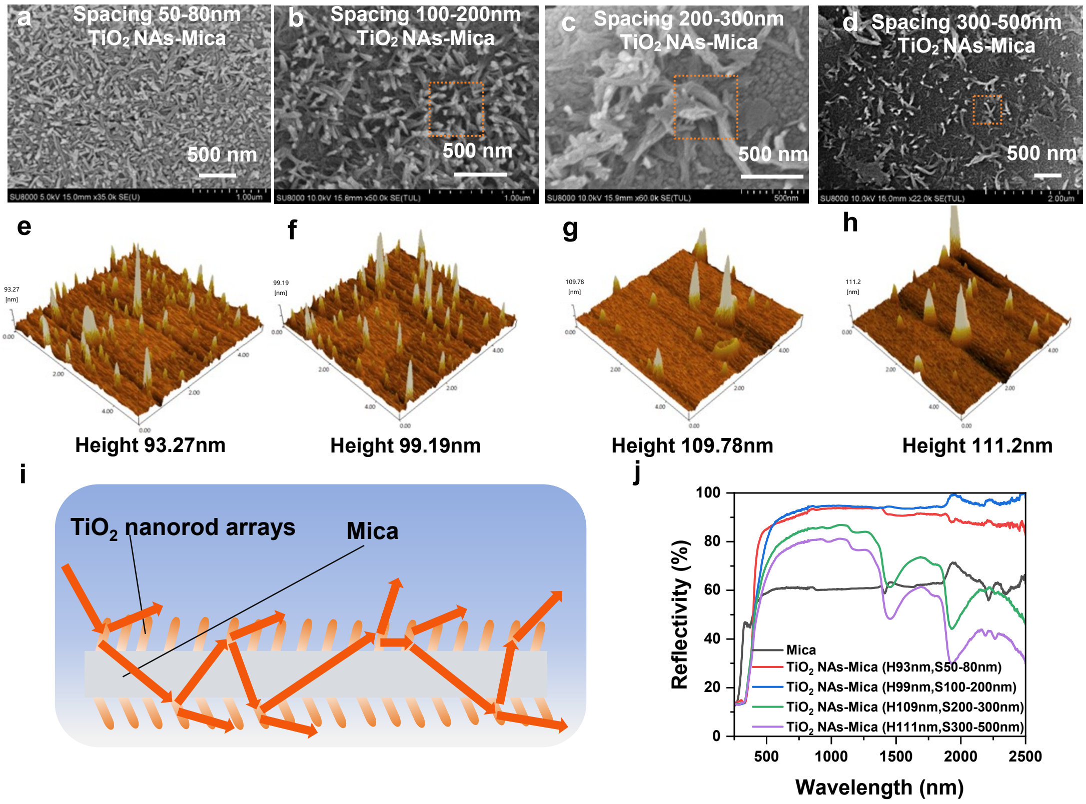

Fig. S2 Solar reflectance at different TiO_2 nanorod spacings and heights (TiO_2 NAs-Mica). (a-d) SEM images of TiO_2 nanorod arrays with different spacings. (e-h) AFM plots of different TiO_2 nanorod arrays heights. (i) Schematic Scattering of TiO_2 NAs-Mica. (j) Solar reflectance of different TiO_2 nanorod arrays.

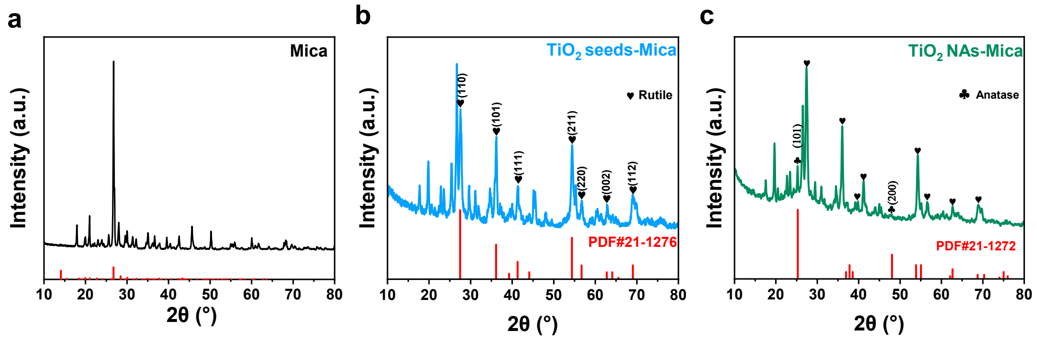

Fig. S3 XRD patterns of (a) Mica, (b) TiO_2 seeds-Mica and (c) TiO_2 NAs-Mica.

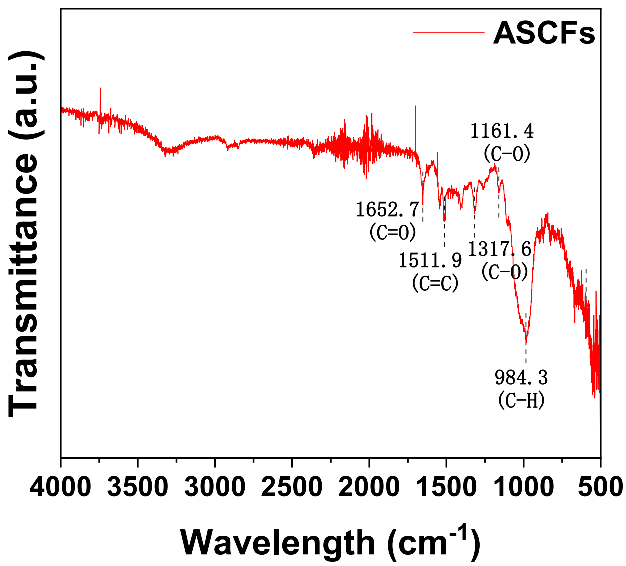

Fig. S4 The FT-IR of ASCFs.

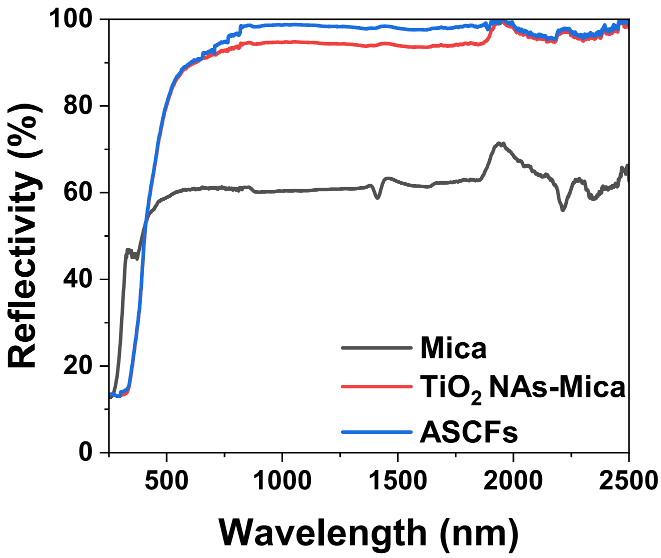

Fig. S5 Solar spectral reflectance of Mica, TiO_2 NAs-Mica and ASCFs.

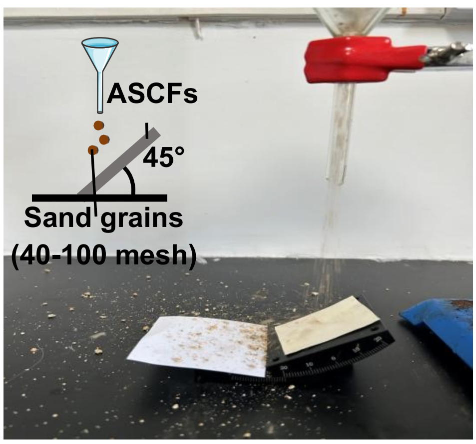

Fig. S6 Scratch resistance test to test durability, the ASCFs was tilted to 45°and abraded on top to simulate falling stones and sand for 60 min.

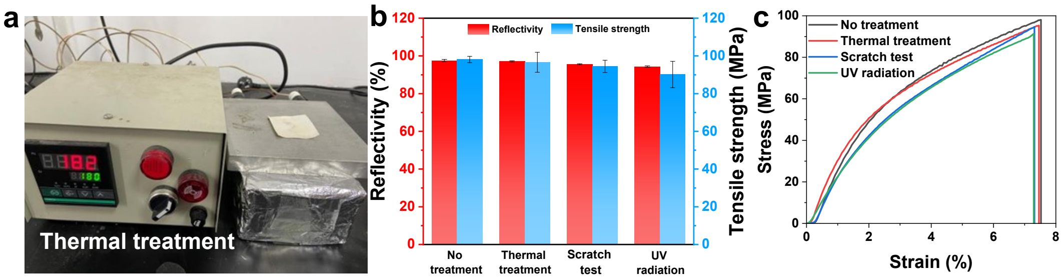

Fig. S7 Environmental durability of mechanical and optical properties for ASCFs. (a) Photographs of thermal treatment (180 °C for 8 h, inset is a photograph of treated ASCFs), (b) The almost unchanged solar reflectance and tensile strength of ASCFs after various extreme weathering treatments. (c) The tensile-stress curve after various extreme weathering treatments.

Table S2 Comparison of mechanical properties and UV resistance of ASCFs with other reported cooling materials

Property	ASCFs (This Work)	TMCP film [8]	CCF film [9]	UPC film [10]
Tensile Strength (MPa)	98	41.7	1.1	Unknown
UV Stability (Reflectance Loss)	3.2% (Sunlight exposure about 280 $MJ\cdot m^{-2}$)	~3.5% (Sunlight exposure about 0.072576 $MJ\cdot m^{-2}$)	~3.4% （Sunlight exposure about 2.592 $MJ\cdot m^{-2}$）	1.3% （Sunlight exposure about 1.296 $MJ\cdot m^{-2}$）

References

1 P. Zhong, X. Ma, X. Chen, R. Zhong, X. Liu, D. Ma, M. Zhang, Z. Li, Nano Energy, 2015, **16**, 99-111.

2 B. Liu, E.S. Aydil, J, Am. Chem. Soc., 2009, **131**, 11, 3985-3990.

3 B. Li, J.M. Wu, T. T. Guo, M.Z. Tang, W. Wen, Nanoscale, 2014, **6**, 3046-3050.

4 J. M. Wu, J. Cryst. Growth., 2004, **269**, 347-355.

5 N. Sutradhar, S.K. Pahari, M. Jayachandran, A.M. Stephan, J.R. Nair, B. Subramanian, H.C. Bajaj, H.M. Mody, A.B. Panda, J. Mater. Chem. A, 2013, **32**, 9122.

6 J. Wu, H. Xue, J. Am. Chem. Soc., 2009, **92**, 2139–2143.

7 P. Li, Y. Liu, X. Liu, A. Wang, W. Liu, N. Yi, Q. Kang, M. He, Z. Pei, J. Chen, P. Jiang, W. Li, H. Bao, X. Huang, Adv. Funct. Mater., 2024, **32**, 6395-6402.

8 P. Zhou, Y. Wang and X. Zhang, Nano Lett., 2024, **24**, 6395-6402.

9 C. Cai, F. Chen, Z. Wei, C. Ding, Y. Chen, Y. Wang and Y. Fu, Chem. Eng. J., 2023, **476**, 146668.

10 W. Sun, X. Tan, G. Qi, X. Yang, W. Hu, W. Jin, Z. Guo, J. Liang, M. Wang and X. Lin, Mater. Today Commun., 2024, **41**, 110797.